Aquat Geochem
DOI 10.1007/s10498-016-9303-5

ORIGINAL PAPER

The Dynamics of Benthic Respiration at a Mid-Shelf Station Off Oregon

Clare E. Reimers[1] · H. Tuba Özkan-Haller[1] · Rhea D. Sanders[1] · Kristina McCann-Grosvenor[1] · Peter J. Chace[1] · Sean A. Crowe[2]

Received: 20 May 2016 / Accepted: 13 September 2016

Abstract Mid-shelf sediments off the Oregon coast are characterized as fine sands that trap and remineralize phytodetritus leading to the consumption of significant quantities of dissolved oxygen. Sediment oxygen consumption (SOC) can be delayed from seasonal organic matter inputs because of a transient buildup of reduced constituents during periods of quiescent physical processes. Between 2009 and 2013, benthic oxygen exchange rates were measured using the noninvasive eddy covariance (EC) method five separate times at a single 80-m station. Ancillary measurements included in situ microprofiles of oxygen at the sediment–water interface, and concentration profiles of pore water nutrients and trace metals, and solid-phase organic C and sulfide minerals from cores. Sediment cores were also incubated to derive anaerobic respiration rates. The EC measurements were made during spring, summer, and fall conditions, and they produced average benthic oxygen flux estimates that varied between −2 and −15 mmol m^{-2} d^{-1}. The EC oxygen fluxes were most highly correlated with bottom-sensed, significant wave heights (H_s). The relationship with H_s was used with an annual record of deepwater swell heights to predict an integrated oxygen consumption rate for the mid-shelf of 1.5 mol m^{-2} for the upwelling season (May–September) and 6.8 mol m^{-2} y^{-1}. The annual prediction requires that SOC rates are enhanced in the winter because of sand filtering and pore water advection under large waves, and it counters budgets that assume a dominance of organic matter export from the shelf. Refined budgets will require winter flux measurements and observations from cross-shelf transects over multiple years.

Electronic supplementary material The online version of this article (doi:10.1007/s10498-016-9303-5) contains supplementary material, which is available to authorized users.

✉ Clare E. Reimers
creimers@coas.oregonstate.edu

[1] College of Earth, Ocean and Atmospheric Sciences, Oregon State University, Corvallis, OR 97331, USA

[2] Departments of Microbiology and Immunology and Earth, Ocean and Atmospheric Sciences, University of British Columbia, Vancouver, BC V6T 1Z4, Canada

Published online: 27 September 2016

Keywords Eddy covariance · Sediment oxygen consumption · Benthic fluxes · Oregon shelf · Deepwater waves

1 Introduction

The continental margin off Oregon and Washington has been described as a slope-dominated margin, critical to the northern California Current ecosystem, where a "substantial part" of the net production is exported seaward of the shelf and therefore not tightly coupled to shelf respiration, benthic fluxes or burial (Jahnke 2010; Nagai et al. 2015). In partial contradiction, the seasonal and interannual variability of dissolved oxygen in shelf bottom waters of this same system has been characterized through coupled biogeochemical and physical modeling as largely controlled by the respiration of sinking detritus with ~70–90 % of the summer production consumed rapidly in the water column and surface sediment layer (Siedlecki et al. 2015). Oregon and Washington shelf sediments are generally slowly to non-accumulating sands or silty muds (Romsos et al. 2007; Wheatcroft et al. 2013), suggesting that over variable timescales nearly 100 % of the detrital organic matter flux to the benthos must be remineralized, or resuspended and exported laterally. Seasonal upwelling is expected to lead to seasonal organic matter inputs that may create seasonal peaks in benthic oxygen consumption and denitrification (Middelburg and Soetaert 2004). Where anaerobic respiration reactions oxidize a significant fraction of the organic carbon flux, the accumulation of reduced compounds as a so-called oxygen debt or oxygen demand units (ODUs) may also affect the variability of benthic oxygen consumption (Pamatmat 1971; Soetaert et al. 1996; Pastor et al. 2011). Here we present new benthic eddy covariance and sediment biogeochemical observations from a study site at 80 m on the Oregon shelf that give greater insight into the dynamics of benthic oxygen consumption and the role of ODUs and physical factors in controlling the sediment oxygen uptake rate. The eddy covariance method was the central focus of this study because it is able to both integrate the effects of spatial heterogeneity and reflect temporal changes in fluxes on timescales of minutes and greater (Berg et al. 2003, 2007; Rheuban and Berg 2013). It has also been proven to be effective in characterizing oxygen fluxes associated with permeable sediments (Berg et al. 2013).

A site at 80 m was targeted to represent the mid-shelf off Oregon because over the past two decades, near-bottom hypoxic conditions have intensified in this zone during the summer upwelling season (Pierce et al. 2012; Peterson et al. 2013; Adams et al. 2013). Our observations reveal a greater complexity of shelf processes than have been simulated in most benthic biogeochemical models that attempt to delineate the factors contributing to hypoxia in the northern California Current system (Connolly et al. 2010; Siedlecki et al. 2015). In particular, variations in bottom boundary layer (BBL) turbulence related to the occurrence of deepwater waves and upwelling versus downwelling conditions are inferred to exert short-term controls on benthic oxygen utilization rates. Winter rates of benthic respiration are also speculated to be higher than summer rates due to enhanced turbulence and organic matter retention on the shelf. The commonality and variability of wave forcings to continental shelf environments worldwide invites further study of their effects on the oxygen and carbon budgets of continental margins.

2 Materials and Methods

2.1 Study Site

This study focuses on an 80-m site (designated as HH80 at 43°55.8′N and 124°14.7′W) located within the broadest section of the Oregon shelf (Fig. 1). Circulation and bottom water characteristics in this shelf area are influenced by seasonal wind-driven Ekman dynamics (i.e., counterclockwise veering, near-bottom transport; Perlin et al. 2007) and flow interactions with Heceta Bank, an offshore rocky bank that also creates important structural habitats for demersal fishes (Barth et al. 2005; Tissot et al. 2008; Siedlecki et al. 2015). Typically, from October through late April, downwelling conditions prevail, leading

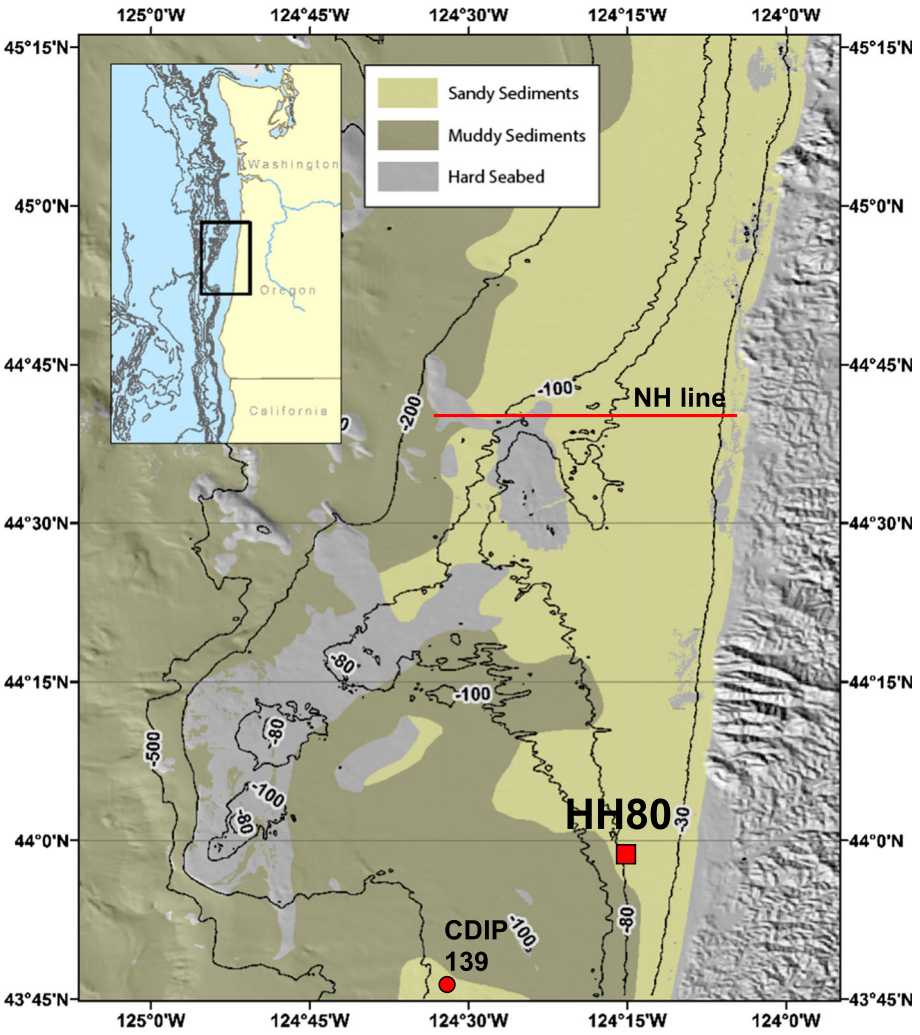

Fig. 1 Map of the central Oregon shelf showing the location of HH80, the CDIP wave buoy (139), the Newport Hydrographic (NH) line, and surrounding seafloor habitats

to offshore near-bottom transport and intense turbulent mixing enhanced by bottom-trapped nonlinear internal waves (Moum et al. 2007). While in summer (May–September) upwelling carries dense near-bottom fluids onshore, there is a greater degree of cross-shelf stratification and less turbulence (Perlin et al. 2005). Wave climatology in this area will be inferred from a wave buoy located at 43°46.0′N and 124°33.0′W. This buoy and its data are maintained by the Coastal Data Information Program (CDIP), station ID = 139 (https://cdip.ucsd.edu).

The surface sediments at HH80 consist of >98 % fine sand and silt. The median grain size of a core sample from 0 to 1 cm was determined to equal 197 μm; permeability (0–20 cm) = 0.7–1.3 × 10^{-12} m^2 (measured on two cores for this study); and organic carbon contents are low (0.2–0.7 wt%; Reimers et al. 2012). Benthic flux measurements assessed in June and August 2009 using chamber incubations yielded oxygen fluxes of −7.2 and −6.7 mmol m^{-2} d^{-1}, respectively, and produced estimates of total carbon oxidized by aerobic respiration and denitrification comparable to other parts of the central Oregon shelf <100 m (Fuchsman et al. 2015). However, it is important to note that these flux determinations were made during periods of bottom water hypoxia, which only occur within the summer upwelling season (Pierce et al. 2012; Peterson et al. 2013). Changing ocean conditions affecting the oxygen content of upwelled waters, changes in the residence time of upwelled waters, and productivity-driven increases in respiration have all been speculated to be contributing to recent increases in Oregon shelf hypoxia (Chan et al. 2008).

2.2 Eddy Covariance Measurements

The measurements and sample collections compiled for this study were made during 5 separate research cruises conducted within 2009, 2011, 2012, and 2013. Eddy covariance (EC) measurements were made at HH80 on each of these cruises, within spring, summer, or fall, using a Nortek Vector Acoustic Doppler Velocimeter (ADV) and oxygen microelectrodes mounted on a sturdy tripod tethered to a surface buoy (as described in Reimers et al. 2012, 2016). Individual deployment records were from 15 to 24 h in duration and during times of both upwelling favorable and unfavorable wind stress (Table 1). During the earliest of these deployments (June 2009), velocity and oxygen measurements were made at 64 Hz in 15-min bursts separated by 5-min gaps as reported in Reimers et al. (2012). The measurements during all subsequent deployments (from October 2011 to July 2013) were made in a continuous mode with the ADV sampling volume situated between 13 and 23 cm above the seabed. Velocities were recorded in the ADV's *xyz* coordinate system (designated as *u, v, w*).

Calibrations of the oxygen microelectrode measurements during each deployment were formed from linear regressions that included zero readings in anoxic dithionite solution recorded on deck and ten discrete in situ readings corresponding to a range of oxygen concentrations recorded by an O_2 optode (Aanderaa Instruments AS, model #3835) (except in 2009; see Reimers et al. 2012 for earlier calibration methods). The optode was attached to a leg of the tripod and sampled at approximately the same height as the microelectrode (±5 cm) at 0.1 Hz. It was also calibrated prior to each deployment in air-saturated seawater and anoxic dithionite solution according to the manufacturer's calibration program that further applies factory temperature coefficients at the salinity of the study site to output oxygen concentrations.

Table 1 EC deployment times, positions, and wind stress conditions

Cruise ID event number	Date (MM/DD/YY) and start time (hh:mm)	Duration (h)	Latitude (N)	Longitude (W)	Water depth[a] (m)	Northward wind stress (N m^{-2})[b]
W0906A-55	06/11/09 15:33	15	43°55.800′	124°14.705	81.6 ± 0.4	−0.024/−0.045
W1110A-44	10/07/11 13:40	18.25	43°55.801′	124°14.711	79.5 ± 0.5	0.018/0.024
OC1204A-80	04/23/12 16:19	18.5	43°55.799′	124°14.699	80.7 ± 0.8	−0.054/−0.011
OC1210A-32	10/10/12 23:44	24	43°55.800′	124°14.691	80.5 ± 0.6	−0.008/−0.005
OC1307A-11	07/09/13 00:00	21	43°55.804′	124°14.697	80.2 ± 0.8	−0.066

[a] Mean ± 1 SD based on the ADV pressure record (m) plus 0.5 m to account for the ADV sensor height above the bottom

[b] Derived from observed winds from NOAA NDBC 46050 off Newport OR for the day(s) over which the deployment occurred (Piece and Barth, http://damp.coas.oregonstate.edu/windstress/)

Seafloor images to accompany the EC measurements were recorded at 15-min intervals throughout the deployments using a digital time-lapse camera (Insite Pacific Inc. Scorpio Plus) and strobe light mounted at the tripod's apex. The best-quality images were observed in October 2012 and July 2013 after overriding an autofocusing feature of the camera that tended to focus on aggregates in suspension within the BBL. From the better photographs, we were able to resolve common epifauna and microtopography features such as bioturbation trials, pits, and mounds.

The procedures used to extract benthic oxygen flux estimates from the EC data were similar to other aquatic field studies (e.g., Lorrai et al. 2010; Holtappels et al. 2013) but tailored to the observed dynamics. (1) Velocities with a beam correlation <50 % were removed and replaced with a cubic polynomial interpolation between neighboring data (this generally altered <1 % of the vertical velocity measurements, except for the record from October 2011 where 4.6 % of the measurements had correlations <50 %), (2) the O_2 and velocity time series were further "cleaned" using the despiking methods of Goring and Nikora (2002) provided this method did not appear to truncate any parts of the velocity records (velocity records from October 2011 and April 2012 showed clear truncation during periods of internal wave variations, so they were not despiked; otherwise, despiking affected <0.5 % of the vertical velocity or oxygen data), (3) the time series were reduced by sequential averaging to 8 Hz, (4) the 8-Hz time series were separated into 15-min segments, (5) each segment was corrected for tilt variations by applying two rotation angles derived by bandpassing the velocity series to isolate wave velocities around the dominant bottom-sensed wave frequency, then evaluating the horizontal angle needed to maximize wave horizontal velocities in the u direction and the vertical angle needed to minimize the standard deviation of the vertical wave velocity (as in Reimers et al. 2012), (6) the corrected instantaneous vertical velocity and oxygen concentration were decomposed into mean and fluctuating components by Reynolds decomposition, $w = \bar{w} + w'$ and $C = \bar{C} + C'$, using a 0.002-frequency filter to remove the mean (after Reimers et al. 2012), (7) a fixed time lag correction (from 0.25 to 1 s, see below) was estimated to account for a delay in the microelectrode response, and (8) after shifting the oxygen series to adjust for the time lag, estimates of the flux of oxygen for each 15-min segment were derived as: $\text{EC Oxygen Flux} = \overline{w'C'}$.

The use of 15-min data segments, rotating coordinates for each segment and applying linear detrending, has been common practice in many prior aquatic EC studies (Berg et al.

2007; Brand et al. 2008; Lorrai et al. 2010; Reimers et al. 2016) and has the effect of filtering out oscillations from w' and C' that occur with periods >15 min (0.0011 Hz) (Finnigan et al. 2003). In this study, we observed that internal wave velocity signatures with periods ~10 min were a common occurrence that created low-frequency variations capable of altering individual EC determinations quite substantially in some cases. Although we have argued previously that over many data segments these low-frequency biases should average out, here we chose instead to exclude these effects by detrending the time series with a 0.002-frequency filter. Compared to linear detrending, the filter altered each deployment's mean EC oxygen flux from as little as -0.1 mmol m^{-2} d^{-1} (October 2011 deployment) to as much as $+6.0$ mmol m^{-2} d^{-1} (June 2009 deployment) (or from 1 to 61 % of reported fluxes) when considering all 5 deployments without excluding any bursts. (Three extreme bursts were excluded in previous analyses of the June 2009 data reported by Reimers et al. 2012).

The choice of time lag correction also affected the derived fluxes. The practice of applying a unique $w'C'$ cross-correlation-based correction for each data segment was rejected over a concern that this can introduce bias that will lead to exaggerated fluxes in the presence of wave motions (Berg et al. 2015). Instead, a fixed lag was assumed that was based on the microelectrode's response time. Time lag shifts from 0 s up to 1 s altered mean flux determinations by as much as -1.9 mmol m^{-2} d^{-1} (April 2012 EC flux, assumed lag = 1.0 s) and as little as -0.3 mmol m^{-2} d^{-1} (July 2013 EC flux, assumed lag = 0.875 s). The other lags applied were 0.375 s for June 2009, 0.25 s for October 2011, and 1.0 s for October 2012 data sets.

2.3 Wave Measurements

Pressure fluctuations associated with surface gravity waves are attenuated with depth, and this attenuation is more pronounced for waves with shorter periods. Hence, signals associated with waves at shorter periods cannot be observed at a near-bottom observation platform at 80 m. Pressure attenuation estimates using linear wave theory suggest that at 80 m depth, only waves at periods >10 s can be observed. Therefore, significant wave height (H_s) estimates derived from our near-bottom instrumentation only capture wave energy at periods larger than 10 s, and the derived values (herein referred to as bottom-sensed wave height) will necessarily be lower than the significant wave height associated with the full wave spectrum.

The bottom-sensed H_s and peak period were estimated using time series of near-bottom pressure (converted to units of depth, m) measured by a sensor integrated with the ADV (and located at the base of the ADV housing) for each 15-min EC data segment. The 15-min estimates were later averaged to produce each deployment mean. The estimation method for the bottom-sensed H_s is based on relating the pressure signal at each frequency with the associated surface wave amplitude at that frequency using the pressure response factor estimated using linear wave theory (Dean and Dalrymple 1992). For comparison purposes, the wave height over the same range of periods (>10 s) was also computed for the nearby CDIP station 139 using a software script available on request from the CDIP data server (https://cdip.ucsd.edu) to separate sea and swell heights with a designated swell cutoff (= 10 s). We assumed station HH80 would experience the same monthly average wave climatology as CDIP station 139.

2.4 Water Column Measurements

The hydrographic properties of the water column at HH80 were characterized by making a CTD-rosette cast at the start of each EC lander deployment period and by making one or two repeat casts before recovery. The CTD package was equipped with additional sensors, including probes for O_2 (SBE 43) and transmissometry (Chelsea/Seatech/Wetlab CStar). The CTD was lowered to within 2–4 m of the seafloor and three 10-L Niskin bottles tripped in a rapid sequence. Generally, each of these bottles was subsampled aboard ship for O_2, nutrients, and particulate organic C and N (POC/PN) concentrations (see Reimers et al. 2012 for methods). The CTD sensor data were processed using the Sea-Bird SEASOFT software and laboratory calibration files. Here we focus on reporting 0.25-dbar average density profiles (expressed as sigma-theta, σ_θ) and bottom water POC concentrations from the CTD-rosette casts.

2.5 Sediment and Pore Water Sampling

During each of the cruises, surface sediment cores were collected from HH80 using either a multi-corer (Ocean Instruments MC-800) or a frame-mounted hydraulically dampened single gravity corer (described in Reimers et al. 2012). Selected cores in tubes pre-drilled with sampling ports were subsampled for pore water chemistry using rhizon samplers (Rhizosphere Research Products B.V.)(Seeberg-Elverfeldt et al. 2005). Generally, approximately 10 ml of pore water was collected in syringes at intervals of 1–2 cm to 30 cm depth. Pore water splits for trace metals were stored at 4 °C and acidified to pH < 2 within a week of sample collection. Additional sample aliquots were frozen at sea and saved for nutrient analyses. Analytical methods used for reported constituents are as described in Abbott et al. (2015).

Pore water O_2 profiles were measured with microelectrodes in situ at a depth resolution of 0.125 mm successfully during the April 2012 and July 2013 cruises. Typically, four O_2 microelectrodes were utilized per deployment, but breakage rates were high due to the sediment coarseness and crabs or other fauna (Reimers et al. 2012).

Core incubations were performed during the October 2011 and July 2013 cruises. All incubated cores (inner diameters of 5.2 cm in October, and 9.6 cm in July) were subsampled from longer and wider multi-corer or hydraulically dampened gravity corer cores and carefully sealed with tops having double o-ring seals and a centered magnetic stir bar rotating in the overlying water under the control of an outer magnet turned by an electric motor. In October 2011, N_2 production rates were estimated by amending the overlying water of three intact cores with $^{15}N\text{-}NO_3^-$ (Nielsen 1992; Christensen et al. 2000). Rates of sediment oxygen utilization were estimated for the same cores from overlying water oxygen concentrations measured using a Pre-Sense optode, at the start and end of the tracer incubations. Sulfate reduction rates were measured using the ^{35}S technique (Fossing and Jørgensen 1989) on a single separate core (2.6 cm inner diameter) subsampled to 20 cm depth. Acid Volatile Sulfide (AVS) and Chromium Reducible Sulfide (CRS, i.e., pyrite) were measured on the same core (Fossing and Jørgensen 1989). In July 2013, three cores were incubated to measure sediment oxygen utilization as above, and nutrient fluxes and the efflux of total CO_2 were also measured. Total CO_2 concentrations were measured using the flow-injection method of Hall and Aller (1992) (average precision of triplicate measurements ± 0.1 mM). All core incubations were maintained under refrigerated conditions at ~ 8 °C.

3 Results

3.1 Eddy Covariance and Water Column Measurements

The five eddy covariance time series and associated CTD profiles measured for this study give snapshots of properties affected by the dynamic processes within the BBL of the Oregon shelf. Although these measurements were made in different years, our objective in this section is to examine these data in a seasonal context with the intent to understand the factors that may control benthic respiration rates. We will characterize conditions of Ekman transport, turbulent mixing, wave motions, and organic matter inputs that may create patterns of variable oxygen flux.

3.1.1 Seasonal Observations

From this point forward, results are presented by order of the calendar month of observation. The April 2012 measurements represent the earliest conditions captured, and they correspond to the very beginning of a spring transition to upwelling conditions when the vertical structure of the water column shows a near-bottom increase in σ_θ (Fig. 2) but not the signature high densities of upwelled source waters ($\sigma_\theta \sim 26.5$, Adams et al. 2013). Horizontal velocities and oxygen concentrations measured over 18.5 h show dramatic variability due to the arrival of a group of nonlinear internal waves (Fig. 3). Resultant 15-min EC fluxes are affected by these dynamics, showing fairly consistent fluxes over the first 5 h of the deployment, while later fluxes oscillate more widely as colder and more oxygen-depleted bottom water is carried over the site with the velocity pulses.

The June and July observations correspond to periods with pronounced upwelling conditions, the coldest, densest bottom waters, and hypoxia. However, the dynamics captured in these two EC time series are very different, with a 15-s swell and nonlinear internal waves creating large velocity pulses in the June 2009 data set (Fig. 4), while component velocities are consistently <5 cm s^{-1} during the July 2013 observations (Fig. 5). Most of the variation in flow and bottom water oxygen seen in the July 2013

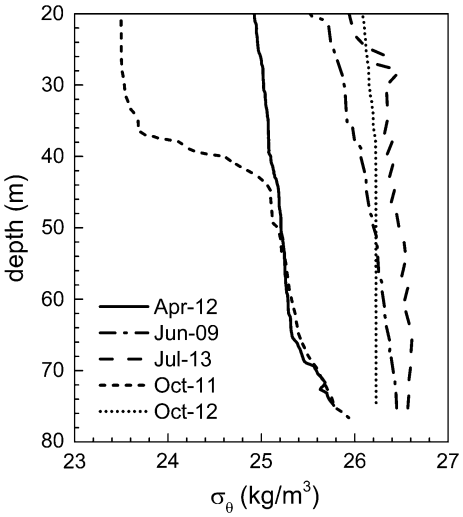

Fig. 2 Vertical profiles of σ_θ derived from CTD casts made near the beginning of each EC lander deployment at HH80

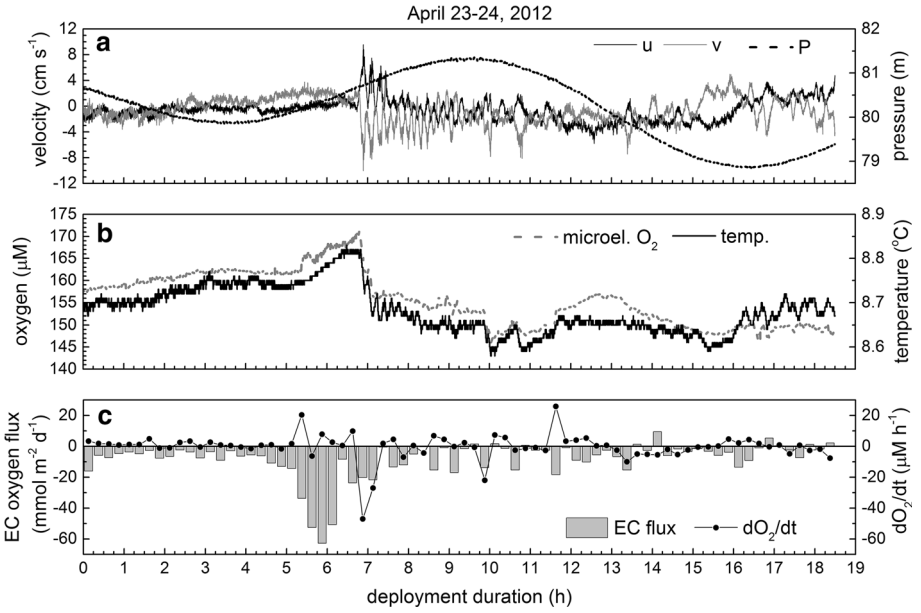

Fig. 3 **a** Time series of horizontal velocity components and pressure (10-s ADV averages) from the EC lander deployment in April 2012. **b** Time series of oxygen (10-s microelectrode averages) and temperature (measured at 0.1 Hz by the optode). **c** EC oxygen fluxes derived from 8-Hz data and overlain with the change in O_2 over time derived for the same 15-min segments

observations appears to be tidally driven. This deployment also displays the lowest and least variable EC oxygen fluxes.

October 2011 and October 2012 measurements are also unique (Figs. 6, 7). The October 2011 measurements were made under the strongest downwelling wind conditions (Table 1) and when there was the most vertical structure in the bottom boundary layer σ_θ profile (Fig. 2). The October 2012 measurements were made during the fall transition that occurred later than in 2011 (Pierce and Barth, wind stress products, http://damp.coas.oregonstate.edu/windstress/index.html). Both October time series show stronger oscillatory motions from surface waves than the other data sets. However, 5 h into the 2012 deployment, a pronounced internal solitary wave appears to transport colder more oxygen-depleted bottom water over the site. This event adds transient storage and advective components to the EC oxygen flux, making 3 of the 15-min flux estimates highly variable. In contrast, a more gradual and prolonged change in the bottom water oxygen (and temperature) is observed in the 2011 time series. This change also adds to the EC oxygen flux variance (Holtappels et al. 2013). Such non-steady-state conditions appear to be the norm on the Oregon shelf (Figs. 3, 4, 5, 6, 7). We have found it difficult to justify excluding some segments of data with such transient variations and not others, so below we will continue to consider all measurements.

3.1.2 Forcing Factors

A comparison of the EC oxygen fluxes observed at HH80 reveals that mean values range from -2.2 to -14.6 mmol m^{-2} d^{-1} (Fig. 8a). Figure 8a also compares median flux

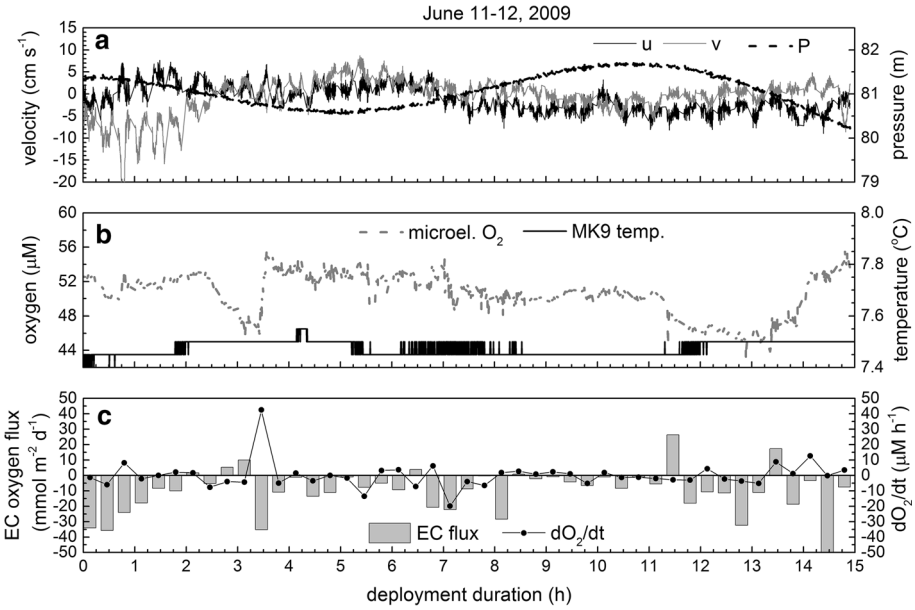

Fig. 4 Same parameters as Fig. 3 except displaying June 2009 measurements. During this deployment, EC measurements were collected in 15-min bursts separated by 5-min gaps. No optode was used, but temperature was monitored with a Wildlife Computers MK-9 sensor (resolution ±0.05 °C) as previously reported in Reimers et al. (2012)

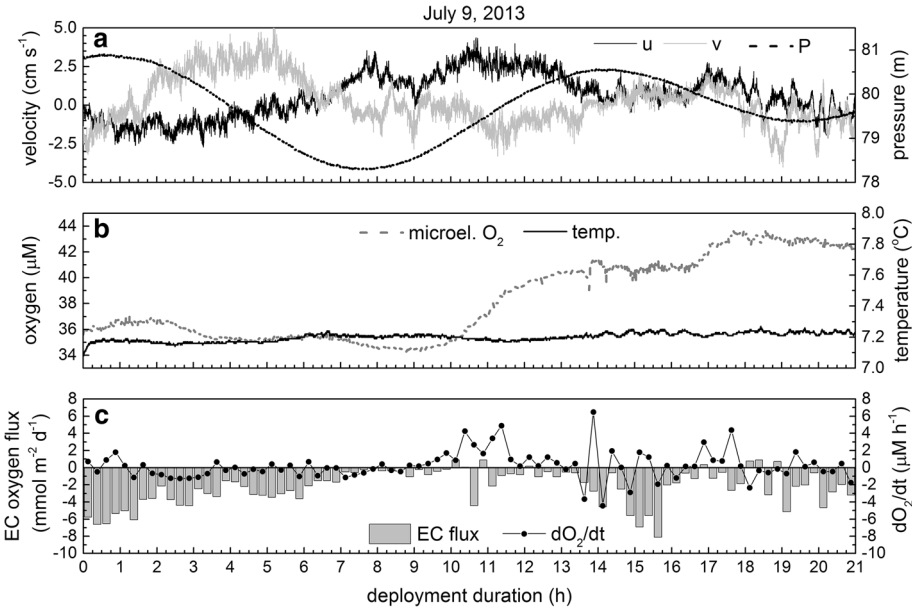

Fig. 5 Same as Fig. 3 except displaying July 2013 measurements

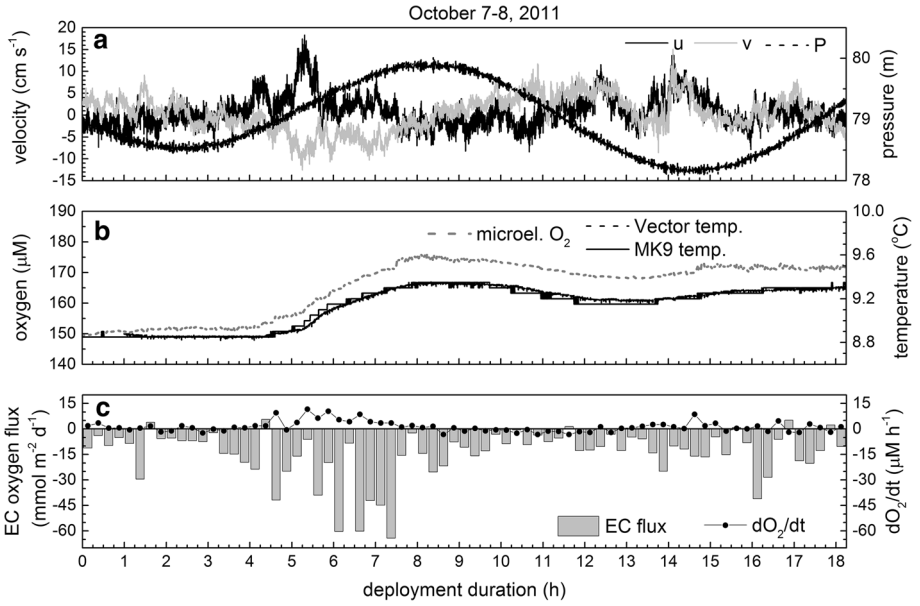

Fig. 6 Same as Fig. 3 except displaying October 2011 measurements. Here, two alternate temperature records from the Vector and the Mk9 sensor are displayed

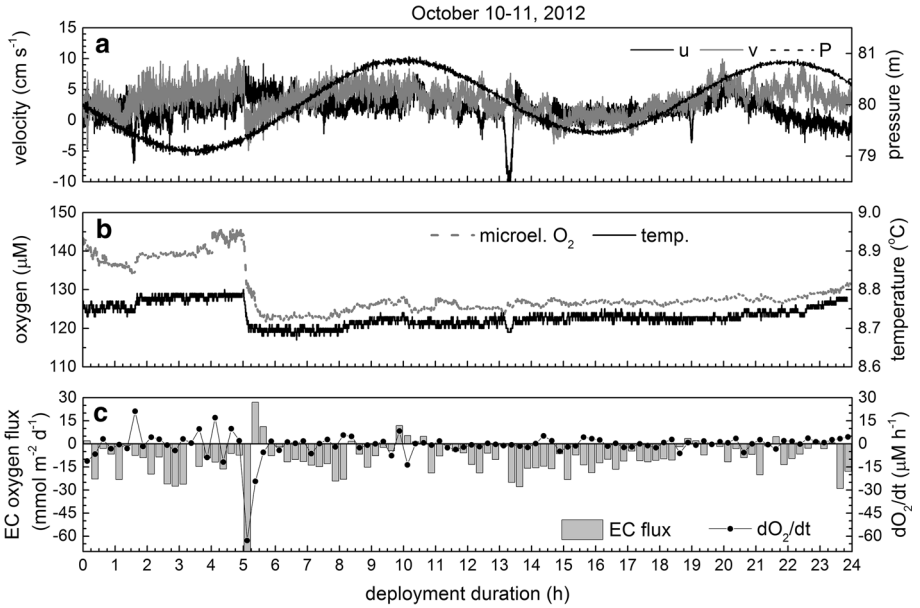

Fig. 7 Same as Fig. 3 except displaying October 2012 measurements

values, the values that bracket 25 and 75 % of the burst estimates, and ±1 SD around each mean. The estimate that appears most different from the others is derived from the July 2013 deployment. Factors that may explain the observed flux differences are compiled

in panels b–f in Fig. 8. Chemical factors considered are the bottom water oxygen concentration (Fig. 8b) that is expected to impact diffusive exchange rates at the seabed (Cai and Sayles 1996), and the particulate organic C concentration in bottom water samples (Fig. 8c) that should increase with higher carbon rain rates. Physical characteristics are parameterized by showing the total kinetic energy $\left(\mathrm{TKE} = \frac{1}{2}\left(\overline{u'u'} + \overline{v'v'} + \overline{w'w'}\right)\right)$ for all deployments at the ADV measurement positions (Fig. 8d), flow speeds (Fig. 8e), and the H_s of surface waves detected in the near-bottom pressure time series of the ADV (Fig. 8f).

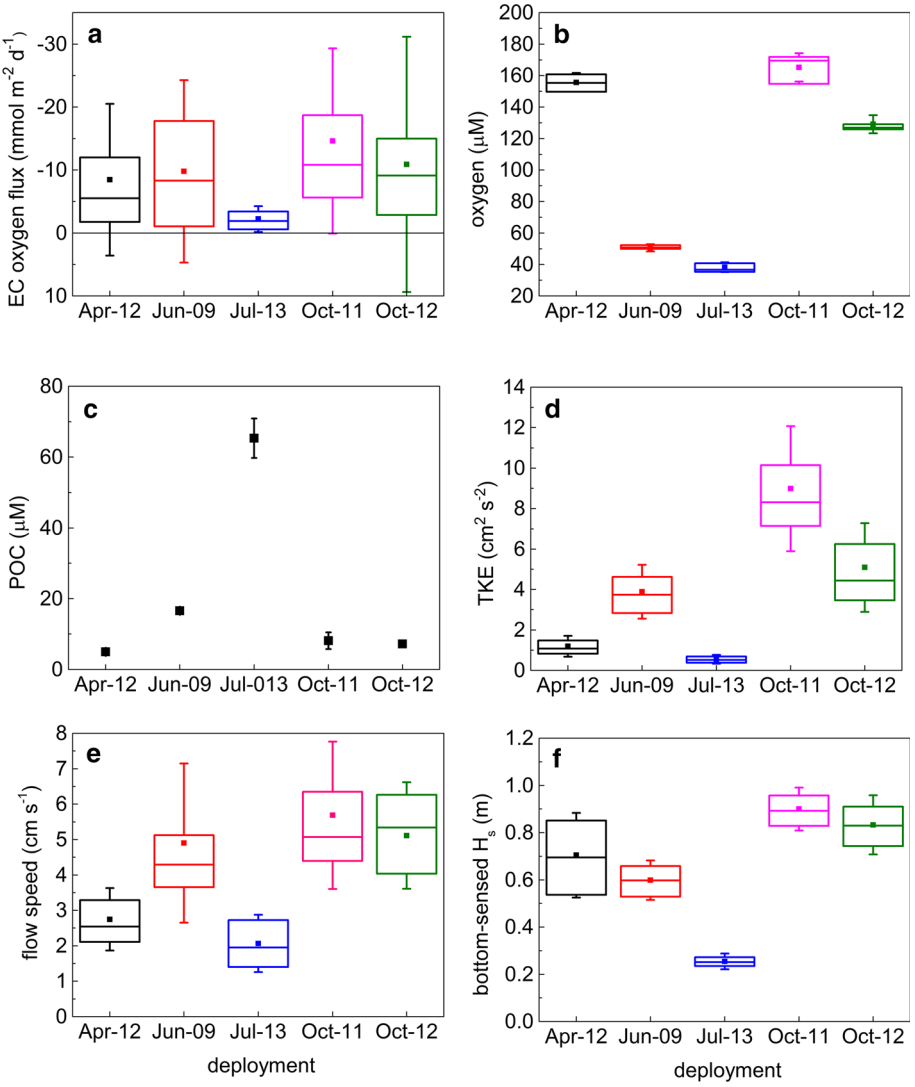

Fig. 8 **a** Comparison of EC oxygen fluxes between deployments and arranged seasonally. For each deployment, the mean of all 15-min bursts is shown as (*square*), *bars* represent ±1 SD about the mean, boxes enclose 25–75 % of the flux variability, and the horizontal line depicts the median. Similarly, in b. oxygen as measured by the EC microelectrode, c. POC concentrations from rosette bottles, z = 3–4 m, **d** turbulent kinetic energy (TKE) for $z = \sim 0.2$ m (ADV sampling height), **e** flow speeds (ADV sampling height), and **f** bottom-sensed significant wave height (H_s) estimated from the near-bottom pressure record

Friction velocities were also derived using the EC method as $u_* = \left|\overline{u'w'}\right|^{1/2}$ (Inoue et al. 2011) but are not plotted because of patterns similar to the other physical factors. Several sediment oxygen consumption models discussed below treat an enhanced diffusion coefficient, as proportional to friction velocity.

A simple cross-correlation analysis between means suggests that it is the physical drivers that explain most of the variance in the EC fluxes between deployments (Table 2). The parameter giving the most significant correlation is the bottom-sensed H_s, suggesting wave-induced advection at the sediment surface enhances sediment oxygen fluxes (Huettel and Webster 2001).

3.2 Oxygen Penetration Depth and Anaerobic Respiration

When the input rate of organic carbon to the seafloor is high enough to promote anoxic mineralization below an interfacial oxic zone, SOC can result from both the direct aerobic mineralization of reactive organic matter and the re-oxidation of reduced solutes and mineral phases that have accumulated as products of anaerobic pathways of organic matter degradation. In seasonally hypoxic systems, the buildup of reduced substrates has been characterized as a sediment "oxygen debt", and this debt is commonly repaid, at least partially, when water column oxygen levels are re-elevated and/or oxygen penetration into the sediment is enhanced by biological or physical mixing (Pamatmat 1971).

During the five sampling periods at HH80, oxygen profiles of high quality were measured on only two occasions successfully with microelectrodes in situ (Fig. 9). Under the assumption that the observed O_2 gradients include a "diffusive sublayer" that extends above the sediment–water interface on the order of 0.5 mm (Jørgensen 2006), these measurements show O_2 penetration extended to $\sim$7 mm in April 2012 but was only to $\sim$1.5 mm under the hypoxic conditions in July 2013. Down-core pore water constituent profiles at different times verify the buildup of reduced products in the deeper sediment (e.g., Fe^{2+} and NH_4^+) (Fig. 10) due to the common diagenetic sequence of organic C oxidation reactions (Aller 2014). These profiles, a separate AVS profile (reported within Supplementary Materials), and visual features of the sediment cores themselves also suggest that physical mixing, or bioturbation, affects the redox state of the surface sediments regularly. Thus, this area of shelf appears capable of accumulating reduced solutes susceptible to re-oxidation when advective processes enhance oxygen transport into the sediment column. It may also exhibit enhanced anaerobic metabolism under periods of higher organic carbon fluxes.

Table 2 Comparison of EC oxygen fluxes between deployments (left 3 columns) and measures of linear correlations between the mean of forcing factors and the mean EC flux (right 3 columns)

deployment	mean EC flux (mmol $m^{-2}d^{-1}$)	SD between bursts	correlation factor to mean EC flux	Pearson corr.	significance
April 2012	-8.5	12.1	bottom water oxygen	-0.71	0.18
June 2009	-9.8	14.5	POC	0.85	0.066
July 2013	-2.2	2.1	TKE	-0.90	0.039
October 2011	-14.6	14.7	flow speed	-0.90	0.037
October 2012	-10.9	20.3	sig. wave height	-0.95	0.014
			friction velocity	-0.76	0.13

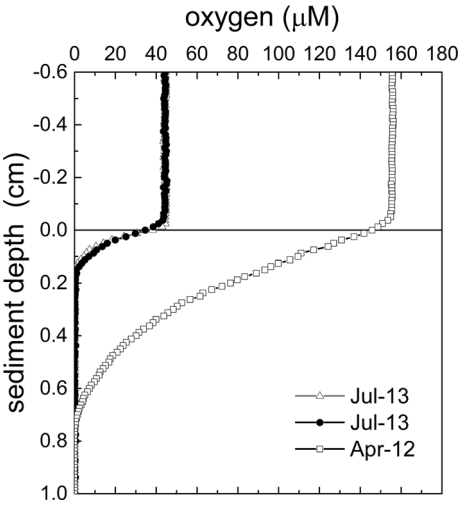

Fig. 9 Profiles of oxygen measured in situ across the sediment–water interface with microelectrodes at HH80

To assess rates of anaerobic carbon degradation, core incubations were conducted both in October 2011 and July 2013. Although the methods were not identical and replication limited, results tallied in Table 3 indicate comparable anaerobic respiration rates. Somewhat surprisingly, core oxygen uptake rates in July 2013 were unusually low, even though in manipulating the cores the overlying bottom water oxygen concentrations were elevated

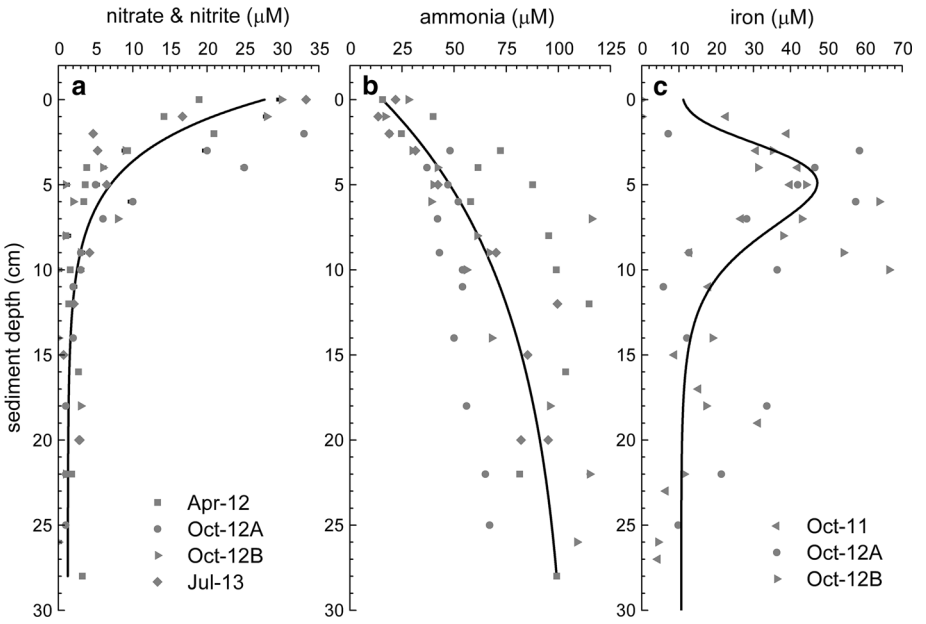

Fig. 10 Pore water constituent data from six different cores sampled with rhizons. One core was sampled on each cruise except in October 2012 when two were sampled. Lines show representative curve fits to all data points (**a** uses an exponential fit, **b** an asymptotic fit, and **c** a peak extreme function). A measured redox species not shown is dissolved manganese. This is because it never exceeded 5 μM

Table 3 Core incubation fluxes and estimates of organic carbon degradation rates by anaerobic respiration processes at HH80

Abbreviation	Flux or rate	October 2011	July 2013
OF	O_2 flux (mmol O_2 m^{-2} d^{-1})	-19.0 ± 14.5 ($n = 3$)	-1.45 ± 0.66 ($n = 3$)
NP	N_2 production (mmol N m^{-2} d^{-1})	3.3 ± 0.2 ($n = 3$)	nd
SR	Sulfate reduction (mmol S m^{-2} d^{-1})	1.9 ($n = 1$)	nd
TCF	Total CO_2 flux (mmol C m^{-2} d^{-1})	nd	5.7 ± 2.0 ($n = 3$)
NF	NO_3^- flux (mmol N m^{-2} d^{-1})	nd	-0.71 ± 0.08 ($n = 3$)
AF	NH_4^+ flux (mmol N m^{-2} d^{-1})	nd (assumed $\sim$ 0)	-0.07 ± 0.005 ($n = 3$)
AnC	Anaerobic C_{ox} (mmol C m^{-2} d^{-1})[a]	5.5	5.7
AC	Aerobic C_{ox} (mmol C m^{-2} d^{-1})[a]	12.7	$\sim$0

Values listed are means $\pm$ 1 SD; *nd* not determined

[a] Derived from the stoichiometry of organic matter oxidation reactions assuming that

(1) AnC + AC = TCF

(2) AnC = 106/94.4 (NP) + 106/53(SR)

(3) AC = 106/118[-OF-2(16/106 (TCF) − AF)]

to values of $\sim$140 μM at the start of each core incubation (see Online Resource 1). Additionally, it appears all oxygen consumption by the July cores can be attributed to ammonia oxidation. This could occur if the ammonia diffusive supply from subsurface sediment equilibrated to equal the oxygen supply established by the gentle stirring of the overlying water in the cores. Little to no aerobic carbon oxidation is also consistent with shallow O_2 penetration (Fig. 9) and with ammonia concentrations in the overlying water being high at the start of the incubations (Online Resource 1).

Oxygen uptake rates by cores incubated in October 2011 showed a wide variability (Table 3) and on average were higher than the EC benthic oxygen flux estimate. This is attributed to bioturbation/bioirrigation influences that were particularly strong in one core (yielding a flux of -35.6 mmol m^{-2} d^{-1}). Surveys of infauna separated from sediment box cores from an area approximately 13 km away at 71–74 m depth show the deposit feeding bivalve *Axinopsida serricata* numerically dominating the infauna (Henkel 2011). Bioturbating demersal organisms visible in bottom photographs taken from the study site include Dungeness crabs, (*Meacarcinus magister*), Pacific Sanddab (*Citharichthys sordidus*), English sole (*Parophrys vetulus*), and a sunflower sea star (*Pycnopodia helianthoides*). The flatfishes were in high density in July 2013 and appeared responsible for creating numerous shallow pits across the sandy sediment surface (Robert and Juniper 2012). Worm tubes, fecal piles, and trails were also visible in bottom photographs.

4 Discussion

The leading reason the eddy covariance method is gaining popularity as a technique for assessing oxygen fluxes at sediment–water interfaces is that the measurements provide an integrated measure of natural exchange processes acting over large areas (10' s m^2; Berg et al. 2007). On the Oregon shelf, this study indicates these processes include advection (e.g., by surface and internal waves), turbulence, bioirrigation/bioturbation, diffusion, and dispersion (emphasized below) occurring under margin-wide upwelling and downwelling

conditions. The results indicate average EC oxygen fluxes at 80 m correlate with code-dependent physical drivers parameterized from near-bottom pressure variations and velocities including deepwater wave heights, flow speed, and turbulent kinetic energy (Table 2). These factors are linked but not exclusively coincident with seasonal Ekman dynamics (i.e., near-bottom transport due to wind-driven upwelling). This is because wave climate depends on winds and storm systems occurring across the North Pacific (Tillotson and Komar 1997; Allan and Komar 2006), and bottom currents are also modulated by diurnal tidal forcing that responds to stratification and shelf width (Erofeeva et al. 2003).

If we accept for initial discussion's sake that the average EC oxygen fluxes measured do accurately reflect real, factor of ~ 7, temporal changes in SOC, we are challenged to explain the linkage between benthic dynamics and sediment oxygen demand, and then to examine the repercussions for seasonal and interannual oxygen variability across this sector of the California Current system. Experimental observations and a conceptual model provided by Güss (1998) offer one plausible explanation and can be illustrated using the in situ O_2 microelectrode profiles shown in Fig. 9. Considering cases of sandy sediments supporting respiration without bioturbation, Güss (1998) presented a form of Fick's first law of diffusion to predict oxygen fluxes as:

$$O_2 \text{ Flux} = -D_{\text{eff}} \frac{\mathrm{d}C}{\mathrm{d}z}\Big]_{z=0}$$

where D_{eff} is an effective exchange coefficient that combines the influences of molecular diffusion and dispersion. Dispersion is perceived as a type of small-scale mixing that extends from just above the sediment–water interface where viscous forces have dampened turbulent mixing, to a sediment depth ($z = l_{\text{disp}}$) that depends on the sediment particle size (d_{p}) and the dynamics at the bed (often parameterized in models using the friction velocity, u_*). This zone is also called a Brinkman layer (Boudreau 1997). In reality, how dispersion depends on velocities above an uneven sediment–water interface and on grain size(s) is not well known, and estimates of D_{eff} derived from flux measurements and models may include small-scale advection, ripple migration, and bioirrigation effects as well (McGinnis et al. 2014).

The gradient across what was interpreted as a diffusive sublayer within the April 2012 O_2 profile (Fig. 9) predicts a diffusive oxygen exchange rate $= -2.5$ mmol m^{-2} d^{-1}, whereas the measurements in July 2013 indicate a diffusive flux $= -2.9 \pm 0.1$ mmol m^{-2} d^{-1} (Table 4 summarizes these calculations). "Dispersion" might therefore explain roughly 71 % of the benthic oxygen exchange rate during the April deployment period, implying D_{eff} ($z = 0$) is 3.4 times D_{mol}. Dispersion rates under the more turbulent conditions observed in June 2009, October 2011, and October 2012 are presumed to have been proportionally greater and to have shifted the O_2 penetration deeper than the ~ 7 mm observed in April.

In July 2013, the average EC oxygen flux (Table 2) is nearly equal to the calculated diffusive flux, suggesting hydrodynamic conditions were not energetic enough to drive

Table 4 Parameters applied in diffusive oxygen exchange rate calculations

Month	D_{mol} (cm^2 s^{-1})	DBL thickness (mm)	dC/dz (μmol cm^{-4})	Diffusive O_2 flux (mmol m^{-2} d^{-1})
April 2012	1.42×10^{-5}	0.375	−0.203	−2.5
July 2013	1.34×10^{-5}	0.25	-0.252 ± 0.011	-2.9 ± 0.1

significant dispersion. The full EC record from July shows (1) a near absence of oscillatory motions stemming from surface waves and (2) bottom currents that never exceeded horizontal speeds of 5.3 cm s^{-1}. At times within the July observations (e.g., between deployment hours 13 and 17), flow speeds dipped below 2 cm s^{-1} consistently (Figs. 5, 8). Brand et al. (2008) observed at flow speeds <2 cm s^{-1} turbulence levels can be insufficient to drive a steady EC flux, causing the EC technique to temporarily underestimate the SOC, especially if the top of the benthic boundary layer is stratified. Indeed, conditions during the first 5 h of the July deployment yielded a higher and more consistent EC flux of -4.0 ± 1.6 mmol m^{-2} d^{-1} at a burst average flow speed of 2.6 ± 0.6 cm s^{-1} and bottom-sensed wave height of 0.28 ± 0.04 m ($n = 20$).

Jahnke et al. (2005) present evidence for enhanced effective diffusion coefficients 2–250 times molecular diffusion, to depths of ≥10 cm, in coarser and shallower water shelf sediments from the South Atlantic Bight. This enhanced transport of solutes is attributed to pore water advection and accompanying dispersion driven by both bottom flow over small-scale topographic features (e.g., ripples, fecal piles and depressions) and wave pumping that is expected to intensify together with organic particle filtration rates as a function of decreasing water depth (Huettel and Rusch 2000; Precht et al. 2004; Reimers et al. 2004; Middelburg and Soetaert 2004). Other studies of shelf sediments have drawn similar conclusions; for example, Lohse et al. (1996) portray SOC in the North Sea occurring in two discrete sublayers where oxygen transport in the top layer is enhanced compared to molecular diffusion. McGinnis et al. (2014) also studied benthic oxygen exchange in the North Sea and showed EC oxygen fluxes had a tidal periodicity driven by tidal currents that had a net effect of enhancing pore water diffusivities as an exponential function of shear velocities.

The fine sand sediments at HH80 have permeabilities ($\sim 1 \times 10^{-12}$ m^2) that make them borderline between what has been characterized as bioturbation- versus advection-dominated transport diagenetic regimes (Huettel and Webster 2001; Aller 2014). These sediments also support anoxic respiratory processes that accumulate reduced by-products such as NH_4^+ and Fe^{2+}, AVS and CRS, "ODUs", that appear to be oxidized to a greater extent when the hydrodynamics intensify (e.g., in October compared to July). Thus, hydrodynamic cycles may decouple O_2 consumption from organic carbon inputs (Middelburg and Soetaert 2004). During winter months (that were not sampled here), H_s values average 2–3 m and can reach 7 m, off Oregon (Tillotson and Komar 1997). The extreme events are expected to resuspend surface sediments, create ripples (Komar et al. 1972), and greatly enhance turbulence and O_2 penetration, limiting long-term burial of organic carbon and ODUs. This conclusion is supported by organic carbon and redox-sensitive trace element concentrations (explicitly Mo, U, and V measured to 50 cm depth in a core from HH80) that do not show enrichments (Erhardt et al. 2014) and relatively low AVS and CRS concentrations (Online Reference 1). Therefore, to ultimately arrive at accurate total annual carbon mineralization rates (from a C:O_2 respiratory ratio) for the middle Oregon shelf and to study interannual variability, we will need time series of sediment–water exchange rates of dissolved oxygen that are measured much more often and for longer continuous periods than in this study. For now, however, we will use a predictive relationship derived from the observed EC oxygen fluxes and bottom-sensed H_s (the physical parameter that had the highest correlation with EC flux) (Fig. 11a). This relationship is assumed to remain linear out to wave heights higher than measured, and to have a zero intercept equal to a diffusion supplied rate of SOC that we equate to 2.5 mmol m^{-2} d^{-1} based on the smallest rate derived from O_2 microprofiles. Integrating over a representative wave climate cycle of analogous swell heights (based on 2012 buoy data, Fig. 11b) implies

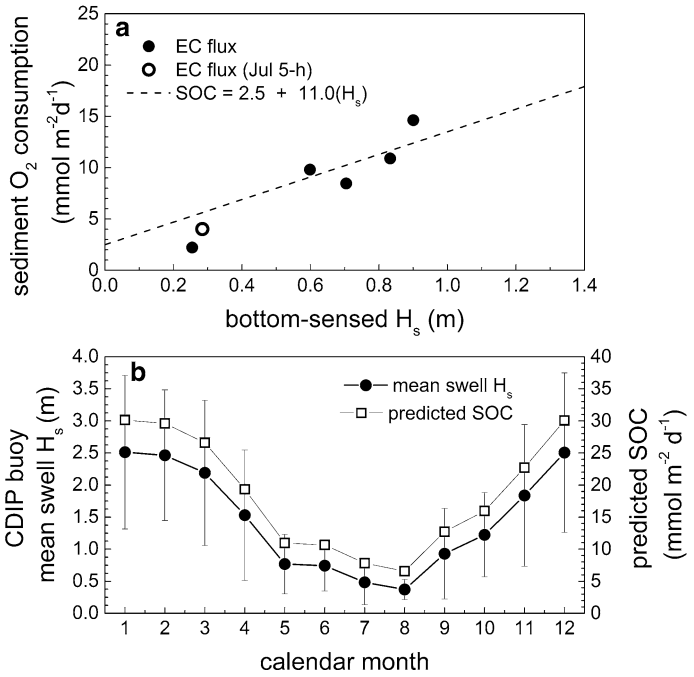

Fig. 11 **a** Relationship between sediment oxygen consumption (SOC) as derived from EC fluxes and bottom-sensed significant wave heights (H_s) at HH80. Solid symbols are deployment means, and the open symbol depicts an alternative estimate for the flux during July 2013 from the first 5 h of the deployment (see text). The predictive equation here was derived by forcing a linear regression through 2.5 mmol m^{-2} d^{-1} (an estimate for a diffusive SOC rate) at zero H_s. The R^2 of this regression = 0.97. **b** Monthly averaged swell significant wave heights (±1 SD) derived from continuously monitored wave spectra with a 10-s cutoff during 2012 from CDIP Station 139. Overlain are predicted SOC rates derived from the swell significant wave heights and the predictive equation in panel **a**

that approximately 1.5 mol O_2 m^{-2} is consumed at the seafloor of HH80 during a typical upwelling season (May–September) and 6.8 mol O_2 m^{-2} could be consumed annually provided there is a sufficient oxygen debt and/or carbon flux to maintain rates through winter months. Predicted SOC rates increase from an August low of 6.6 mmol m^{-2} d^{-1} to 30 mmol m^{-2} d^{-1} in December and January, implying sustained inputs of particulate organic carbon and oxygen via sand filtering and pore water advection (Huettel and Rusch 2000). This seasonal picture is in contrast to seasonal cycles of production inferred from Oregon shelf satellite data and measurements of surface chlorophyll and pCO_2 (Bosch 2002; Evans et al. 2011), and it is in contrast to biogeochemical model predictions that assume rates of water column and benthic respiration respond rapidly to phytodetritus fluxes coupled to summer peaks in primary productivity (as, e.g., in Siedlecki et al. 2015). However, the flux cycle in Fig. 11 could be realistic if an equivalent fraction of particulate organic carbon is retained via along shelf advection and short-term burial in the shelf environment during and after the summer upwelling season (a hypothesis counter to assumptions of major export from the shelf). Additionally, fresh organic matter is likely to be supplied to the benthos through production events throughout the winter (although these rates need documentation). We have observed an equal range of SOC rates at a 30 m site near the NH line (Fig. 1) as reported in McCann-Grosvenor et al. (2014). However, this study too shows only temporal snapshots and lacks winter measurements.

The microelectrodes used to sense oxygen variations for EC flux determinations in this and previous studies have a number of limitations, especially durability and reliability through long-term measurements. Recent research has also identified velocity sensitivities and response lag biases that can introduce error into flux estimates especially under waves (Donis et al. 2015; Holtappels et al. 2015; Berg et al. 2015; Reimers et al. 2016). As indicated in the Methods section above and examined in Reimers et al. (2016), these changeable effects as well as different detrending approaches for acquiring covariances can add or subtract approximately 2–3 mmol m^{-2} d^{-1} to average EC oxygen fluxes measured at sites on the Oregon shelf. A limitation of the EC method at present is there is no certain set of data reduction protocols or corrections for biases under unsteady, mixed wave and current boundary layer flows. There are new optode O_2 sensors, however, that do not exhibit any signal sensitivity to velocities (Berg et al. 2016). Further testing and development of these or other new sensors would benefit future studies of dynamic shelf environments.

Another conundrum in aquatic EC science is how to treat long period variations in horizontal velocities or in mean oxygen concentrations that are independent of the seafloor source or sink (Holtappels et al. 2013; McCann-Grosvenor et al. 2014). The answer given by micrometeorologists is to average EC measurements over periods much longer than the low-frequency motions that generate transient changes in the boundary layer (Finnigan 2004). In other words, transient changes in mean velocities or dissolved oxygen add variability to EC measurements on 15-min timescales, but when integrated over long periods of time, one should derive a flux that accurately represents the seafloor sink or source. In this study, the measurement periods ranged from 15 to 24 h, thus capturing variations due to tides and internal waves. Average EC oxygen fluxes for a given deployment were also similar in magnitude to concurrent core incubation fluxes (October 2011 and July 2013) and in situ benthic chamber measurements made in June 09 (Fuchsman et al. 2015). The drop off in the benthic oxygen flux in July 2013 during a period of little wave activity and low turbulence indicates that the oxygen debt phenomenon described by Pamatmat (1971) is an important regulator of benthic fluxes in this region. This had not been observed in previous studies of the Oregon shelf.

The first paper reporting any in situ benthic flux data for sites on the continental margin off Oregon was by Severmann et al. (2010) followed by Berelson et al. (2013) who focused on benthic iron, oxygen, nitrate, and ammonia fluxes at heavily bioturbated mud sites at 105 and 190 m to the west of HH80. Now through studies at additional sites and across seasons (Reimers et al. 2012; McCann-Grosvenor et al. 2014; Fuchsman et al. 2015), we are beginning to assemble a more complete picture of the factors contributing to spatial and temporal variability in benthic respiration throughout this region.

A goal of many ocean observationalists is to provide, through measurements, enough insight into individual processes and forcing functions to enable realistic models of regional ecosystems. These models may then be applied to determine probable system responses to future climatic forcing (Siedlecki et al. 2015). Benthic respiration parameterizations on continental shelves have been especially challenging because of the need to accommodate over a depth gradient differences in sediment texture, organic matter production/delivery, deposition–erosion cycles, and the active filtering or mixing of sediments by benthic organisms or wave motions, among other factors (Huettel and Rusch 2000; Middelburg and Soetaert 2004). The rates of EC oxygen exchange measured at 80 m inshore of Heceta Bank may be larger than other Oregon shelf locations because of the retentive nature of circulation in this domain (Barth et al. 2005; Siedlecki et al. 2015). Our snapshot views of the oxygen dynamics suggest BBL responses to organic matter inputs

can be delayed and attenuated in summer periods with reduced turbulence, but revived at the end of the upwelling season when the BBL becomes more turbulent due to wave pumping and downslope flow. Deepwater wave motions increase and include more storm events starting in autumn months creating what may be the main driver for temporal variations in benthic oxygen consumption. Wave motions on the Oregon shelf appear as major contributors to near-bottom flow speeds, a related variable that other studies have shown to regulate EC oxygen fluxes to permeable sediments (Berg et al. 2013; McGinnis et al. 2014). Water temperature is not an important variable as in other shelf systems such as the South Atlantic Bight (Jahnke et al. 2005). Whether annual integrated rates of organic matter deposition are balanced by sediment mineralization or unbalanced because of significant export within the BBL during downwelling conditions is still uncertain and may vary with shelf width. Refined budgets will require winter measurements and further study of cross-shelf transects over multiple years.

Acknowledgments This research was supported by the National Science Foundation (NSF) under Grant OCE-1061218. Peter Chace's participation was funded by the NSF Research Experience for Undergraduates (REU) Program under Grant No. NSF OCE-1263349. We are indebted to the marine technicians, officers, and crew of the R/Vs *Wecoma* and *Oceanus* for the execution of the field studies. We also acknowledge contributions at sea from Margaret Sparrow, Katie Watkins-Brandt, Andrea Albright, Shelby LaBuhn, Cody Doolen, Michael Courtney, and Annie Thorp. Pore water iron and nutrient analyses were performed by Jessie Muratli and Joe Jennings in facilities at Oregon State University. Chip Hogue helped to gather and interpret sediment infauna data. Peter Berg and one anonymous reviewer provided helpful manuscript reviews. This paper is dedicated to Rick and Debbie Jahnke whose work and collegiality have shaped the field of benthic biogeochemistry.

References

Abbott AN, Haley BA, McManus J, Reimers CE (2015) The sedimentary flux of dissolved rare earth elements to the ocean. Geochim Cosmochim Acta 154:186–200

Adams KA, Barth JA, Chan F (2013) Temporal variability of near-bottom dissolved oxygen during upwelling off central Oregon. J Geophys Res 118:4839–4854. doi:10.1002/jgrc.20361

Allan JC, Komar PD (2006) Climate controls on US west coast erosion processes. J Coast Res 22:511–529

Aller RC (2014) Sedimentary diagenesis, depositional environments, and benthic fluxes. In: Holland HD, Turekian KK (eds) Treatise on geochemistry, vol 8, 2nd edn. Elsevier, Oxford, pp 293–334

Barth JA, Pierce SD, Castelao RM (2005) Time-dependent, wind-driven flow over a shallow midshelf submarine bank. J Geophys Res Oceans 110:C10S05. doi:10.1029/2004JC002761

Berelson WM, McManus J, Severmann S, Reimers CE (2013) Benthic flux of oxygen and nutrients across Oregon/California shelf sediments. Cont Shelf Res 55:66–75

Berg P, Rϕy H, Janssen F, Meyer V, Jϕrgensen BB, Huettel M, De Beer D (2003) Oxygen uptake by aquatic sediments measured with a novel non-invasive eddy correlation technique. Mar Ecol Prog Ser 261:75–83

Berg P, Røy H, Wiberg PL (2007) Eddy correlation flux measurements: the sediment surface area that contributes to the flux. Limnol Oceanogr 52(4):1672–1684

Berg P, Long MH, Huettel M, Rheuban JE, McGlathery KJ, Howarth RW, Foreman KH, Giblin AE, Morino R (2013) Eddy correlation measurements of oxygen fluxes in permeable sediments exposed to varying current flow and light. Limnol Oceanogr 58:1329–1343

Berg P, Reimers CE, Rosman JH, Huettel M, Delgard ML, Reidenbach MA, Özkan-Haller HT (2015) Technical note: time lag correction of aquatic eddy covariance data measured in the presence of waves. Biogeosciences 12:6721–6735

Berg P, Koopmans DJ, Huettel M, Li H, Mori W, Wüest A (2016) A new robust oxygen-temperature sensor for aquatic eddy covariance measurements. Limnol Oceanogr Methods 14:151–167

Bosch J (2002) Satellite-measured chlorophyll variability within the upwelling zone near Hecata Bank, Oregon. MS Thesis, University of Maine, p 87

Boudreau BP (1997) Diagenetic models and their implementation. Springer, Berlin

Brand A, McGinnis DF, Wehrli B, Wüest A (2008) Intermittent oxygen flux from the interior into the bottom boundary of lakes as observed by eddy correlation. Limnol Oceanogr 53:1997–2006
Cai W-J, Sayles FL (1996) Oxygen penetration depths and fluxes in marine sediments. Mar Chem 52:123–131
Chan F, Barth JA, Lubchenco J, Kirincich A, Weeks HA, Peterson WH, Menge BA (2008) Emergence of anoxia in the California Current large marine ecosystem. Science 319:920
Christensen PB, Rysgaard S, Sloth NP, Dalsgarrd T, Schwaerter S (2000) Sediment mineralization, nutrient fluxes, denitrification and dissimilatory nitrate reduction to ammonium in an estuarine fjord with sea cage trout farms. Aquat Microb Ecol 21:73–84
Connolly TP, Hickey BM, Geier SL, Cochlan WP (2010) Processes influencing hypoxia in the northern California Current system. J Geophys Res Oceans 115:C03021. doi:10.1029/2009JC005283
Dean RG, Dalrymple RA (1992) Water wave mechanics for engineers and scientists. In: Advanced series on ocean engineering, vol 2. World Scientific Publishing, p 353
Donis D, Holtappels M, Noss C, Cathalot C, Hancke K, Polsenaere P, Wenzhoefer F, Lorke A, Meysman FJR, Glud RN, McGinnis DF (2015) An assessment of the precision and confidence of aquatic eddy correlation measurements. J Atmos Ocean Technol 32:642–655
Erhardt AM, Reimers CE, Kadko D, Paytan A (2014) Records of trace metals in sediments from the Oregon shelf and slope: investigating the occurrence of hypoxia over the past several thousand years. Chem Geol 382:32–43
Erofeeva SY, Egbert GD, Kosro PM (2003) Tidal currents on the central Oregon shelf: models, data, and assimulation. J Geophys Res Oceans 108(C5):3148. doi:10.1029/2002JC001615
Evans W, Hales B, Strutton PG (2011) Seasonal cycle of surface ocean pCO_2 on the Oregon shelf. J Geophys Res 116:C05012. doi:10.1029/2010JC006625
Finnigan J (2004) Advection and modeling. In: Lee X, Massman W, Law B (eds) Handbook of micrometeorology. A guide for surface flux measurement and analysis. Kluwer Academic Publishers, Dordrecht, pp 209–244
Finnigan JJ, Clement R, Malhi Y, Leuning R, Cleugh HA (2003) A re-evaluation of long-term flux measurement techniques Part 1: averaging and coordinate rotation. Bound Layer Meteorl 107:1–48
Fossing H, Jørgensen BB (1989) Measurement of bacterial sulfate reduction in sediments: evaluation of a single-step chromium reduction method. Biogeochemistry 8:205–222
Fuchsman CA, Devol AH, Chase Z, Reimers CE, Hales B (2015) Benthic fluxes on the Oregon shelf. Estuar Coast Shelf Sci 163:156–166
Goring DG, Nikora VI (2002) Despiking acoustic Doppler velocimeter data. J Hydraul Eng 128:117–126. doi:10.1061/(ASCE)0733-9429(2002)128:1(117)
Güss S (1998) Oxygen uptake at the sediment water interface simultaneously measured using a flux chamber method and microelectrodes: must a diffusive boundary layer exist? Estuar Coast Shelf Sci 46:143–156
Hall POJ, Aller RC (1992) Rapid, small-volume, flow injection analysis for ΣCO_2 and NH_4^+ in marine and freshwaters. Limnol Oceanogr 37:1113–1119
Henkel SK (2011) Characterization of benthic conditions and organisms on the Oregon south coast: a rapid evaluation of habitat characteristics and benthic organisms at the proposed Reedsport wave park. A report prepared for the Oregon Wave Energy Trust, p 15
Holtappels M, Glud RN, Donis D, Liu B, Hume A, Wenzhöfer F, Kuypers MMM (2013) Effects of transient bottom water currents and oxygen concentrations on benthic exchange rates as assessed by eddy correlation measurements. J Geophys Res Oceans 118:1157–1169
Holtappels M, Christian N, Hancke K, Cathalot C, McGinnis DF, Lorke A, Glud RN (2015) Aquatic eddy correlation: quantifying the artificial flux caused by stirring sensitive O2 sensors. PLoS One 10(1):e0116564
Huettel M, Rusch A (2000) Transport and degradation of phytoplankton in permeable sediment. Limnol Oceanogr 45:534–549
Huettel M, Webster IT (2001) Porewater flow in permeable sediments. In: Boudreau BP, Jørgensen BB (eds) The benthic boundary layer transport processes and biogeochemistry. Oxford University Press, New York, pp 144–179
Inoue T, Glud RN, Stahl H, Hume A (2011) Comparison of three methods for assessing in situ friction velocity: a case study from Loch Etive, Scotland. Limnol Oceanogr Methods 9:275–287
Jahnke R (2010) Global Synthesis. In: Liu KK, Atkinson L, Quiñones R, Talaue-McManus L (eds) Carbon and nutrient fluxes in continental margins. Springer, Berlin, pp 597–615
Jahnke R, Richards M, Nelson J, Robertson C, Rao A, Jahnke D (2005) Organic matter remineralization and porewater exchange rates in permeable South Atlantic Bight continental shelf sediments. Cont Shelf Res 25:1433–1452

Jørgensen BB (2006) Bacteria and marine biogeochemistry. In: Schultz HD, Zabel M (eds) Marine geochemistry, 2nd edn. Springer, Berlin, pp 169–206
Komar PD, Neudeck RH, Kulm LD (1972) Observations and significance of deepwater oscillatory ripple marks on the Oregon continental shelf. In: Swift D, Duane D, Pilkey O (eds) Shelf sediment transport. Dowden, Hutchinson and Ross, Inc, Stroudsburg, pp 601–619
Lohse L, Epping EHG, Helder W, van Raaphorst W (1996) Oxygen pore water profiles in continental shelf sediments of the North Sea: turbulent versus molecular diffusion. Mar Ecol Prog Ser 145:63–75
Lorrai C, McGinnis DF, Berg P, Brand A, Wüest A (2010) Application of oxygen eddy correlation in aquatic systems. J Atmos Ocean Technol 27:1533–1546
McCann-Grosvenor K, Reimers CE, Sanders RD (2014) Dynamics of the benthic boundary layer and seafloor contributions to oxygen depletion on the Oregon inner shelf. Cont Shelf Res 84:93–106
McGinnis DF, Sommer S, Lorke A, Glud RN, Linke P (2014) Quantifying tidally-driven benthic oxygen exchange across permeable sediments: an aquatic eddy correlation study. J Geophys Res Oceans 119:6918–6932
Middelburg JJ, Soetaert K (2004) The role of sediments in shelf ecosystem dynamics. In: Robinson AR, McCarthy J, Rothschild BJ (eds) The sea, volume 13, ISBN 0-471-18901-4, pp 353–373
Moum JN, Klymak JM, Nash JD, Perlin A, Smith WD (2007) Energy transport by nonlinear internal waves. J Phys Oceanogr 37:1968–1988
Nagai T, Gruber N, Frenzel H, Lachkar Z, McWilliams JC, Plattner G-K (2015) Dominant role of eddies and filaments in the offshore transport of carbon and nutrients in the California Current System. J Geophys Res Oceans 120:5318–5341. doi:10.1002/2015JC010889
Nielsen LP (1992) Denitrification in sediment determined from nitrogen isotope pairing. FEMS Microbiol Ecol 86:357–362
Pamatmat MM (1971) Oxygen consumption by the seabed IV. Shipboard and laboratory experiments. Limnol Oceangr 16:536–550
Pastor L, Cathalot C, Deflandre B, Viollier E, Soetaert K, Meysman FJR, Ulses C, Metzger E, Rabouille C (2011) Modeling biogeochemical processes from the Rhône River prodelta area (NW Mediterranean Sea). Biogeosciences 8:1351–1366
Perlin A, Moum JN, Klymak J (2005) Response of the bottom boundary layer over a sloping shelf to variations in alongshore wind. J Geophys Res Oceans 110:C10S09. doi:10.1029/2004JC002500
Perlin A, Moum JN, Klymak JM, Levine MD, Boyd T, Kosro PM (2007) Organization of stratification, turbulence, and veering in bottom Ekman layers. J Geophys Res 112:C05S90. doi:10.1029/2004JC002641
Peterson JO, Morgan CA, Peterson WT, Di Lorenzo E (2013) Seasonal and interannual variation in the extent of hypoxia in the northern California Current from 1998-2012. Limnol Oceanogr 58:2279–2292
Pierce SD, Barth JA, Shearman RK, Erofeev AY (2012) Declining oxygen in the Northeast Pacific. J Phys Oceanogr 42:495–501
Precht E, Franke U, Polerecky L, Huettel M (2004) Oxygen dynamics in permeable sediments with wave-driven pore water exchange. Limnol Oceanogr 49:693–705
Reimers CE, Stecher HA III, Taghon GL, Fuller CM, Huettel M, Rusch A, Ryckelynck N, Wild C (2004) In situ measurements of advective solute transport in permeable shelf sands. Cont Shelf Res 24:183–201
Reimers CE, Özkan-Haller HT, Berg P, Devol A, McCann-Grosvenor K, Sanders RD (2012) Benthic oxygen consumption rates during hypoxic conditions on the Oregon continental shelf: evaluation of the eddy correlation method. J Geophys Res Oceans 117:C02021. doi:10.1029/2011JC007564
Reimers CE, Özkan-Haller HT, Albright A, Berg P (2016) Microelectrode velocity effects and aquatic eddy covariance measurements under waves. J Atmos Ocean Technol 33:263–282. doi:10.1175/JTECH-D-15-0041.1
Rheuban JE, Berg P (2013) The effects of spatial and temporal variability at the sediment surface on aquatic eddy correlation measurements. Limnol Oceanogr Methods 11:351–359
Robert K, Juniper SK (2012) Surface-sediment bioturbation quantified with cameras on the NEPTUNE Canada cabled observatory. Mar Ecol Prog Ser 453:137–149
Romsos C, Goldfinger C, Robison R, Milstein R, Chaytor J (2007) Development of a regional seafloor surficial geologic habitat map for the continental margins of Oregon and Washington, USA. In: Todd BJ, Greene G (eds) Mapping the seafloor for habitat characterization. Geological Association of Canada Special Paper 47, pp 209–234
Seeberg-Elverfeldt J, Schülter M, Feseker T, Kölling M (2005) Rhizon sampling of porewaters near the sediment-water interface of aquatic systems. Limnol Oceanogr Methods 3:361–371
Severmann S, McManus J, Berelson WM, Hammond DE (2010) The continental shelf benthic iron flux and its isotope composition. Geochim Cosmochim Acta 74:3984–4004

Siedlecki SA, Banas NS, Davis KA, Giddings S, Hickey BM, MacCready P, Connelly T, Geier S (2015) Seasonal and interannual oxygen variability on the Washington and Oregon continental shelves. J Geophys Res Oceans 120:608–633. doi:10.1002/2014JC010254

Soetaert K, Herman PMJ, Middelburg JJ (1996) Dynamic response of deep-sea sediments to seasonal variations: a model. Limnol Oceanogr 41:1651–1668

Tillotson K, Komar PD (1997) The wave climate of the Pacific Northwest (Oregon and Washington): a comparison of data sources. J Coastal Res 13:440–452

Tissot BN, Wakefield WW, Hixon MA, Clemons JER (2008) Twenty years of fish-habitat studies on Heceta Bank, Oregon. In: Reynolds JR, Greene HG (eds) Marine habitat mapping technology for Alaska, Alaska Sea Grant college program, University of Alaska Fairbanks, pp 203–217. doi:10.4027/mhmta.2008.15

Wheatcroft RA, Goñi MA, Richardson KN, Borgeld JC (2013) Natural and human impacts on centennial sediment accumulation patterns on the Umpqua River margin, Oregon. Mar Geol 339:44–56